AMSE JOURNALS-AMSE IIETA publication-2017-Series: Advances B; Vol. 60; N°1; pp 140-160
Submitted Jan. 2017; Revised March 15, 2017, Accepted April 15, 2017

An Automated Schematic Method Based on Dynamic Grid for Service Area Map

* Tan Zuofei, ** Li Shenglin*, *** Wang Zhaoxia, **** Guo Yudong, ***** Wei Xiaofu

*Department, Logistics Information & Logistic Engineering, Logistic Engineering University of Tan Zuofei
China, Chongqing, (tan.zuo.fei@163.com)
** Department, Logistics Information & Logistic Engineering, Logistic Engineering University of Li Shenglin
China, Chongqing, (492739390@qq.com)
*** Department, Logistics Information & Logistic Engineering, Logistic Engineering University of Wang Zhaoxia
China, Chongqing, (492739390@qq.com)
**** Department, Logistics Information & Logistic Engineering, Logistic Engineering University of Guo Yudong
China, Chongqing, (gyd116046122@163.com)
***** Department, Logistics Information & Logistic Engineering, Logistic Engineering University of Wei Xiaofu
China, Chongqing, (1514347327@qq.com)

Abstract

This paper presents an automatic mechanism for service area maps. This method of mechanism includes a set of strategies to simplify the outlines of public facilities. A number of constraints are defined, which are used to keep the directions and topology layout of maps. Other constraints are used to keep the relative locations among facilities and lines in themselves. Those constraints construct a classic linear programming to solve the optimal value of the objective function consisting of dynamic grid radiuses. This paper shows the method through a street map, and verifies the method both in a qualitative evaluation and a quantitative evaluation. The experimental results

indicate that the method realizes the map-schematic process and reduces topological confliction. Moreover, the method has better schematization and similarity for original map.

Key words

Schematization; Service area map; Dynamic grid; Relative location maintaining; Linear programming; Fractal dimension

1. Introduction

Maps are widely used in transportation, urban planning, public administration, industrial management and so on. For different purposes, there are various visual objects which may be extracted from satellite imagery, 3D realistic scene or CAD image [1]. Essentially, those visual objects are just some simulations for material objects. So the detail of material objects are attenuated in different extent when they turn into visual objects. The 3D realistic scene as a kind of visual object can keep detail as much as possible for some safeguard managements [2]. But too much detail in a small area of a map will lead to serious visual clutter which affects legibility severely in some missions. This argument is based on the following 2 points to consider. On one hand, maps only need highlight specific information and omit the secondary ones for the specific missions [3]. On the other hand, according to Gestalt psychology, mental operation and memory is limited, so human tend to understand visual objects into simple, regular structure. Filtered cartographic messages would relieve human's cognitive load [4]. For example, CAD drawing and 3D drawing with much detail will hinder maintainer's visual for public equipment inspection or property administrator's visual for property management. To improve such situation, the displayed graphic must be simplified and schematized.

In this paper, it propose a schematic method to deal with some missions like public equipment inspection, property management. Those missions' visual requirement is slightly different from traditional schematic missions such as search for different kinds of network lines. The method includes not only schematization for linked lines, but also schematization for closed not linked objects with each other.

2. Related works

There were some important works by predecessors to deal with line and area schematization. The most famous schematic map is Harry Beck's artificial drawing London subway map which only focused on link relationship among points but ignored the point coordinates [5].

More researches gave much attention on line segment simplification such as Neyer's chain simplification algorithm [6], Merrick's importance-based algorithm [7], Cabello's equivalent topology algorithm [8, 9] and Barkowsky's discrete curve evolution algorithm [10]. Furthermore, Oke et al. employed multiobjective mixed integer programming to build the direction and location constraints, which can generate a group of strict 8-directions graphic but lead to a great distorting. These methods let most discrete curves become fewer line segments but didn't take topology similarity with original graphic into consideration. Our method also uses a programming method to get the optimal result. But in order to get a similar location relation, we choose linear programming. Other researchers focused on iterative refinement methods. For instance, Ware [12] and Anand [13] both gave their attention on Douglas-Peucker algorithm and employed simulated annealing algorithm to find a schematic solution, Hong et al. [14] tried to schematic network based on a spring algorithm, Stott [**Erreur ! Source du renvoi introuvable.**] constructed a multi-condition constraint to solve schematic-layout problem, Wolff et al. [16] optimized network layout by mixed integer programming to make the layout satisfy a hard constraint and a soft constraint. However, these methods were not optimal results and have fussy preference. In other aspect, cartology researchers tried to simplify buildings in urban city, Regnauld [**Erreur ! Source du renvoi introuvable.**] employed a generalization strategy to squaring building walls, J.H. Haunert et al. [18] held an edges-minimizing method to simplify building outline, Li Zhenhua [19] figured out a displacement algorithm to solve conflicts between roads and buildings. Such methods all researched the buildings themselves and relation between buildings and roads, but did not give focus on the complex public equipment.

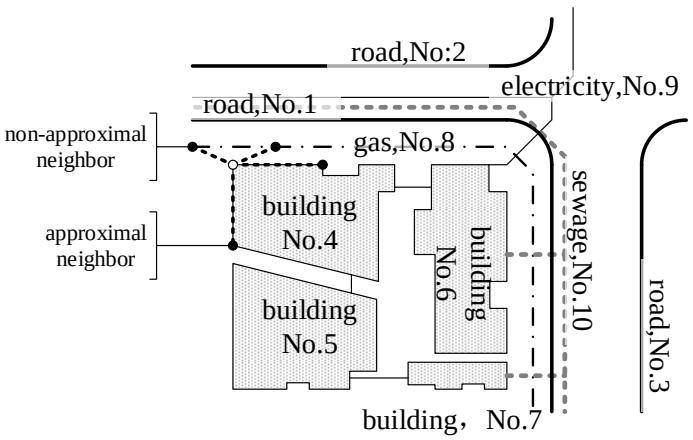

Fig.1. Facility points in schematic service area map

3. Schematic method

In this section, we discuss the basic methods of the schematic service area maps. Firstly, a direction constraint is given to distort the map; secondly, a method we call dynamic grid based on Stott's point-move rectangle will to be introduced; thirdly, a location constraint between approximal points in a facility is proposed; fourthly, a project to keep the relative location among different independent facilities is presented.

In our method, each independent facility such as road, building, underground water main, has its serial number, just like in Arcgis, each facility has its unique property. Each facility is made by a set of points. These points know which facility they belong to and the class of the facility is, which point is their approximal neighbor, which point is their non-approximal neighbor. In the schematic service area maps, the approximal neighbor point is important to keep the basic structure of a facility, and the non-approximal neighbor point is significant to keep the structure of a heap of facilities in a limited area. The above recommendation can be shown in figure 1. Section 3.1 mention a direction constraint. Based on the direction constraint, a set of constraint formulas would be deduced in the following sections. These constraints are relative to any point and its approximal neighbor or non-approximal neighbor point. When all points with their neighbor points can satisfy these constraints, a linear programming with these constraints can be used for schematic requirement.

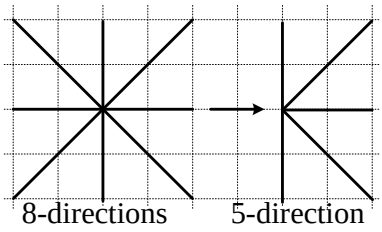

Fig.2 Direction setting in our method

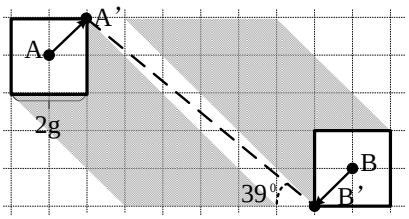

Fig.3 Limitation of Stott's method

3.1 Direction constraint

In recent studies, some researchers indicate that 8-directions of a map has more advantage on legibility and aesthetics than other direction schematic map [20]. 8-directions means that each edge of a graph in map need to be drawn horizontally, vertically or diagonally at 45^0. So in our method, we also choose the 8-directions as the direction constraint. However, in algorithm implementation, atan() and atan2() functions return values in different intervals [-pi/2, pi/2] and [-pi, pi]. So the 2 functions above cannot express the range from 0^0 to 360^0 and then the 8-directions need to change. As we choose atan() as the available function, these intervals determining 8-directions which

includes 0^0, 45^0, 90^0, 135^0, 180^0, 225^0, 270^0, 315^0 and 360^0 change into 5-directions schematic, including -90^0, -45^0, 0^0, 45^0, 90^0, which is shown in figure 2. In a way, the two kinds of directions are the same, the angles in the second and third quadrant can be replaced by the angles in the first and fourth quadrant. So we also call the 5-directions 8-directions in our paper.

3.2 Dynamic grid method

In Stott's automatic metro map method, each point embedded on an integer rectangle grid. The grid's side length is fixed *lg* to reduce the number of potential locations of metro stations. Such a method would reduce calculated amount in its hill climbing optimizer and make the distance of 2 adjacent stations be more regular. However, this method might cause a problem, as is shown in figure 3. Suppose the *lg=2g*, if a point *A* tries to get the 45^0 to the point *B*, it should move its location to an appropriate location. In the limited integer rectangle grid, point *A* can just get closer to this direction, not reach.

So we give points the dynamic non-integer rectangle grids, making them move to the right direction to meet the aesthetic quality of map. Firstly, there are some variables in the following subsections: the (x_i, y_i) are the original coordinates of point *i*, which are known quantities, the R_i is point *i*'s dynamic grid radius, which is an unknown quantity, the (X_i, Y_i) are point *i*'s distorted coordinates, which are unknown quantities. With those variables, a set of constraints below has been built and then the original graphic will be distorted into an 8-directions one. In the following sections, we also use those variables to construct new orientation and location constraints.

0^0 direction constraint criterion

When the two adjacent points' direction closes to horizontal direction, there are two possibilities, which are shown in figure 4(a) and figure 4(b). Due to the points' dynamic non-integer rectangle grids, the inequation $R_A \le R_B$ or $R_B \le R_A$ can be correct. The new distorted points' coordinates Y_A, Y_B should be in the shaded pattern area, which is named overlapping region in figure 4.

In order to get the overlapping region, the unknown coordinates Y_A, Y_B of two adjacent points need to satisfy the following inequations:

$$y_A - \frac{R_A}{2} \le Y_A \le y_A + \frac{R_A}{2} \tag{1}$$

$$y_B - \frac{R_B}{2} \le Y_B \le y_B + \frac{R_B}{2} \tag{2}$$

Because the angle of point *A* and *B* to the horizontal direction is nearly to 0^0, then line *AB* should change its angle to 0^0, so satisfying the following equation:

$$Y_A = Y_B \tag{3}$$

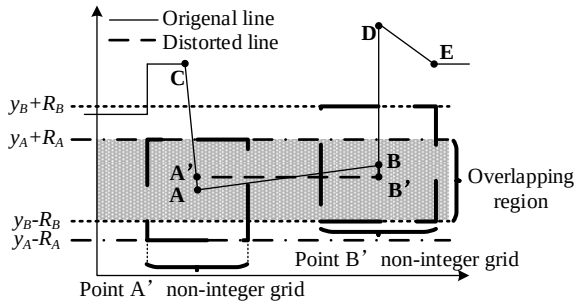

(a) Absolute overlapping relation

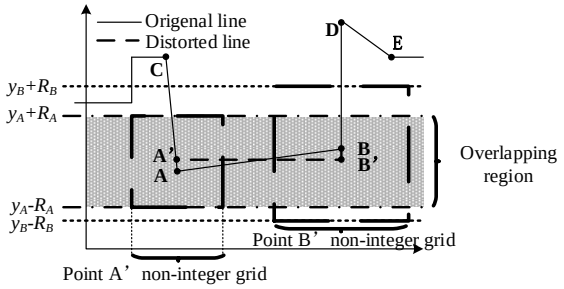

(b) Non-absolute overlapping relation

Fig.4 Example of 0^0 direction constraint

Then plug equation 3 into inequations 1 and 2, no matter absolute overlapping relation and non-absolute overlapping relation, the following inequations are holding:

$$y_A - \frac{R_A}{2} \le y_B + \frac{R_B}{2} \tag{4}$$

$$y_B - \frac{R_B}{2} \le y_A + \frac{R_A}{2} \tag{5}$$

Then we can see in figure 4, the area defined by inequations 4 and 5 is the overlapping region. So we can deduce the constraint condition:

$$\begin{cases} -Y_A - R_A/2 \le -y_A \\ Y_A - R_A/2 \le y_A \\ -Y_B - R_B/2 \le -y_B \\ Y_B - R_B/2 \le y_B \\ Y_A - Y_B = 0 \\ R_A \ge 0, R_B \ge 0 \end{cases} \tag{6}$$

±90^0 direction constraint criterion

When the two adjacent points' direction closes to vertical direction, there are two possibilities. The angle range of the two points [67.5^0~112.5^0] or [-112.5^0~-67.5^0] are equivalent to [67.5^0~90^0] and [-67.5^0~-90^0]. The deduction of constraint criterion is just like the 0^0 constraint, the only different place is coordinates. So the overlapping region is in this area:

$$x_A - \frac{R_A}{2} \le x_B + \frac{R_B}{2} \tag{7}$$

$$x_B - \frac{R_B}{2} \le x_A + \frac{R_A}{2} \tag{8}$$

And the constraint condition is:

$$\begin{cases} -X_A - R_A/2 \le -x_A \\ X_A - R_A/2 \le x_A \\ -X_B - R_B/2 \le -x_B \\ X_B - R_B/2 \le x_B \\ X_A - X_B = 0 \\ R_A \ge 0, R_B \ge 0 \end{cases} \tag{9}$$

±45^0 direction constraint criterion

In this situation, the constraint condition is not only relative to a single coordinate, but also relative to another coordinate. Firstly, as is shown in figure 5, to achieve the goal of 45^0 direction between two neighbor points, each point need to stay in the overlapping area of 45^0. The limitation dotted line's formula *f(x)* can be expressed as:

$$Y = X + b \tag{10}$$

Among them, parameter b is the vertical axis value of the intersection between formula $f(x)$ and Y-axis. For example in figure 5, point A's upper limitation formula $f_{max}(x)$ is:

$$y_A + R_A/2 = x_A - R_A/2 + b_{\max} \tag{11}$$

So the $b_{\max}$ can be expressed as following:

$$b_{\max} = y_A - x_A + R_A \tag{12}$$

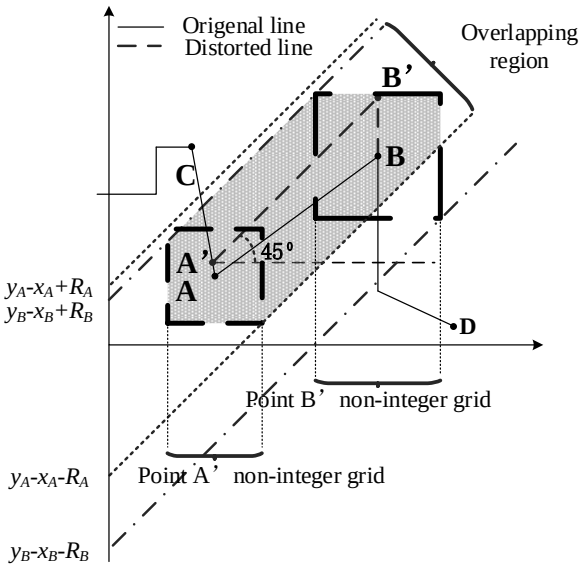

(a) Absolute overlapping relation

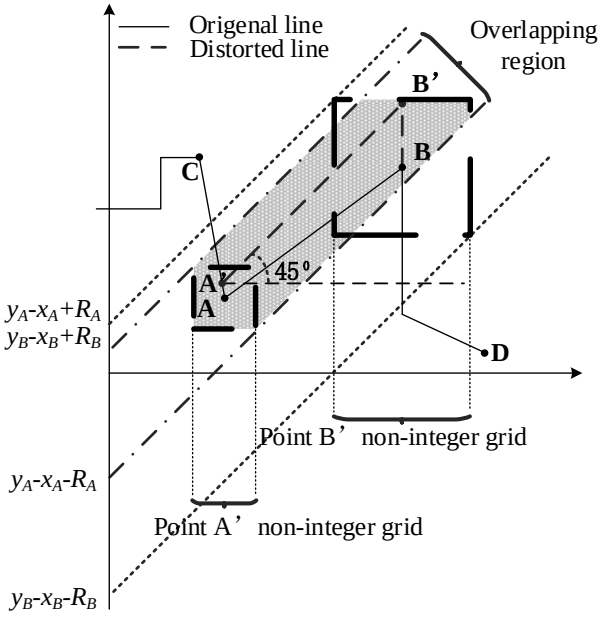

(b) Non-absolute overlapping relation

Fig.5 Example of 45^0 direction constraint

And then we can get the lower limitation $f_{min}(x)$ is:

$$y_A - R_A/2 = x_A + R_A/2 + b_{\min} \tag{13}$$

And $b_{\min}$ is:

$$b_{\min} = y_A - x_A - R_A \tag{14}$$

So point A can satisfy such inequations:

$$\begin{cases} b_{\min} \le b_A \le b_{\max} \\ Y_A = X_A + b_A \end{cases} \tag{15}$$

And then, combining formula 11~14, we can get such an inequation:

$$y_A - x_A - R_A \le Y_A - X_A \le y_A - x_A + R_A \tag{16}$$

Similarly, point B can satisfy:

$$y_B - x_B - R_B \le Y_B - X_B \le y_B - x_B + R_B \tag{17}$$

In order to make point A and point B keep on 45^0 direction, such two points must obey the following equation:

$$Y_B - X_B = Y_A - X_A \tag{18}$$

And there also exists two situations just like the 0^0 direction, shown in figure 5(a) and (b), according to the formulas above, the two situations always obey these inequations, and the overlapping region is always embedded in such area:

$$y_B - x_B - R_B \le y_A - x_A + R_A \tag{19}$$

$$y_A - x_A - R_A \le y_B - x_B + R_B \tag{20}$$

Then we can get the constraint condition is:

$$\begin{cases} X_A - Y_A - R_A \le x_A - y_A \\ -X_A + Y_A - R_A \le y_A - x_A \\ X_B - Y_B - R_B \le x_B - y_B \\ -X_B + Y_B - R_B \le y_B - x_B \\ X_A - Y_A - X_B + Y_B = 0 \\ R_A \ge 0, R_B \ge 0 \end{cases} \tag{21}$$

Secondly, if an edge with two points closer to the -45^0 direction, which means that the edge's angle range is from -22.5^0 to -67.5^0. On this occasion, the -45^0 direction's constraint condition can be deduced like the 45^0 direction above. So the constraint is following:

$$\begin{cases} -X_A - Y_A - R_A \le -x_A - y_A \\ X_A + Y_A - R_A \le y_A + x_A \\ -X_B - Y_B - R_B \le -x_B - y_B \\ X_B + Y_B - R_B \le y_B + x_B \\ X_A + Y_A - X_B - Y_B = 0 \\ R_A \ge 0, R_B \ge 0 \end{cases} \tag{22}$$

3.3 Specific orientations maintaining among a facility

After the dynamic grid method, each point can be limited in a set of banding areas by some directions. However, it cannot keep the location among adjacent points completely with such constraints. Such constraints only generate horizontal, vertical and diagonal direction relation between 2 adjacent points, not describe the specific orientations. The specific orientations of points are not only decided by their adjacent points but also relative to their dynamic grid range. Stott's method gave a fixed grid and a quadrant rule to keep the specific orientations. Our method is different with the 'Stott' method slightly, we also employ the quadrant rule, but adopt a constraint

relation between dynamic coordinates and dynamic grid range. This constraint can avoid points far away from their original locations.

With the constraint below, the right location maintaining can be illustrated in figure 6(c). But without such a constraint, edges adjacent might become self-intersection, out of ordering and far away from the original position, as is shown in figure 6(b). With the quadrant rule, point *E* can be the upper side of point *D* in figure 6(c) like the original graph in figure 6(a), no intersection and no out-ordering occur. After those explanations, we can figure out constraint conditions in different directions. In the inequations below, the capital letters are variable and the lowercase letters are constant which the original coordinates are.

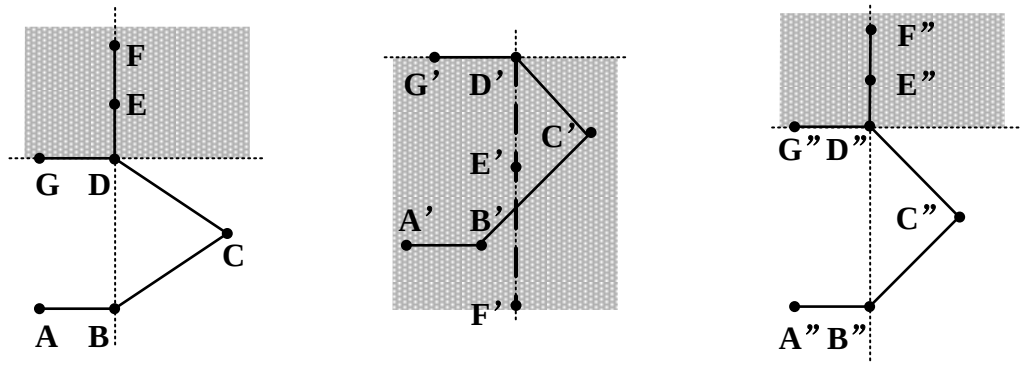

(a)The original graph (b)The false orientation (c)The right orientation

Fig.6 Specific orientation maintaining in a facility

Firstly, due to the distorted edge is horizontal, the 0^0 direction constraint could not consider the Y-axis coordinates of two approximal points. So the condition is:

$$\begin{cases} X_A - X_B \le 0, x_A \le x_B \\ X_B - X_A \le 0, x_B \le x_A \\ -X_A - R_A/2 \le -x_A \\ X_A - R_A/2 \le x_A \\ R_A \ge 0 \end{cases} \tag{23}$$

Secondly, the $\pm 90^0$ direction constraint can ignore the X-axis, so the condition is:

$$\begin{cases} Y_A - Y_B \le 0, y_A \le y_B \\ Y_B - Y_A \le 0, y_B \le y_A \\ -Y_A - R_A/2 \le -y_A \\ Y_A - R_A/2 \le y_A \\ R_A \ge 0 \end{cases} \tag{24}$$

Thirdly, the $\pm 45^0$ direction constraint can either choose the X-axis coordinate or the Y-axis coordinate to get conditions. This time we choose X-axis coordinate and this is just the same to inequations 23 above.

3.4 Relative location maintaining among independent facilities

If a facility changes its shape into 8-directions, it may conflict with other facility. In recent researches, all emphasizes are focus on the topologic relations among points with connection, in other words, within a single facility. These schematic maps are widely used in route map, road network and so on. But for service area maps, the non-approximal points in other facilities need to be considered before schematizing. For example, in a service area map for maintenance and planning purposes, utility companies not only need to achieve a schematic map to keep legibility but also need to know the relative location among facilities to find the target object in a short time.

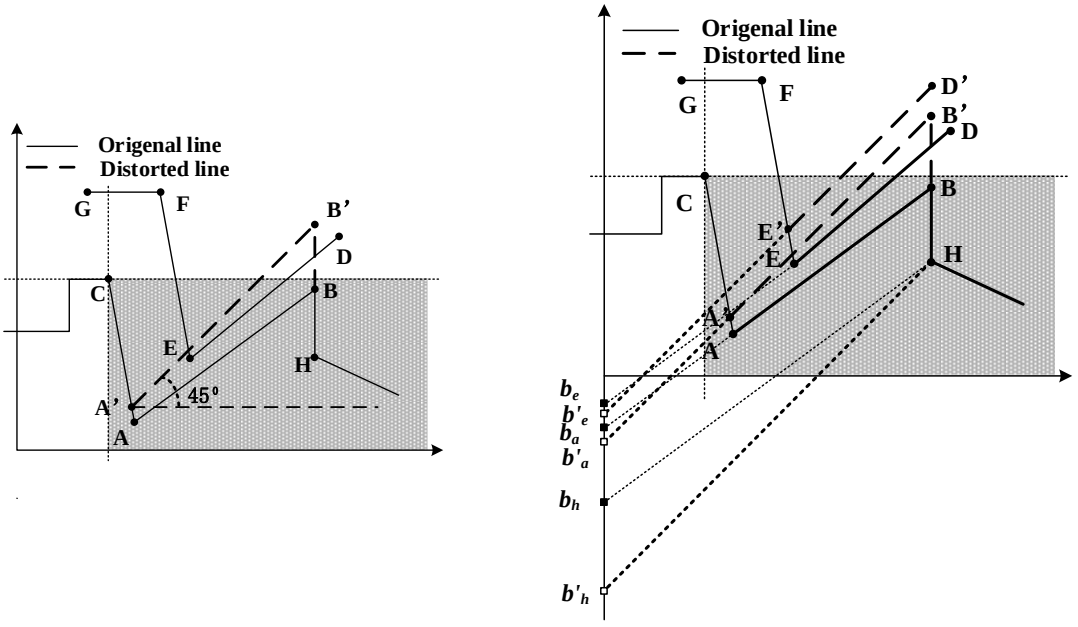

(a) The problem of point-to-point relation (b) The independence maintaining method

Fig.7 relative location maintaining among independent facilities

In approximal network, each point can keep the relative location with other adjacent points by relative location constraint. But such point-to-point relation method cannot solve the edge-to-point relation problem, which problem is shown in figure 7(a). Point *A* is in the fourth quadrant of point *C*, when the edge of *AB* tries to distort its direction to 45^0 direction, its new location may be the dash line. For point *A*, its relative location to its approximal point *C* doesn't change after distorting. But for the non-approximal point *E* and point *D*, their relative locations to edge *AB* has changed from upper side to the lower side. This would change the facility-to-facility relative location at a macro level. Before distorting, the graph *CAB* is separated to the graph *GFED*, after distorting, the two graphs intersect. However point *E*'s relative location to point *C* and point *A* is also not changed. So we need a new method to deal with such problem.

In order to deal with such problem, two new auxiliary lines need to be painted for each adjacent edge. As is shown in figure 7(b), for any point *A*, find the adjacent edges ***E***(*AB,AC...*) consisted of its self and its adjacent points; then get the closest non-approximal points at both sides of the adjacent edge, point *E* and point *H* are such non-approximal points in figure 7(b); finally paint the line cross these two points with the same slope of object adjacent edge *AB*, tiny dotted lines cross points *E* and *H* are in figure 7(b). We can get the tiny dotted lines' functions as following:

$$\begin{cases} y_A = \dfrac{y_A - y_B}{x_A - x_B} x_B + b_a \\ y_E = \dfrac{y_A - y_B}{x_A - x_B} x_E + b_e \\ y_H = \dfrac{y_A - y_B}{x_A - x_B} x_H + b_h \end{cases} \tag{25}$$

Due to points *A*, *E* and *H*'s coordinates are known, the intersection coordinates of Y-axis can be expressed as:

$$\begin{cases} b_a = y_A - \dfrac{y_A - y_B}{x_A - x_B} x_A \\ b_e = y_E - \dfrac{y_A - y_B}{x_A - x_B} x_E \\ b_h = y_H - \dfrac{y_A - y_B}{x_A - x_B} x_H \end{cases} \tag{26}$$

So we can get the relative location before distorting map:

$$b_h \le b_a \le b_e \tag{27}$$

And the relative location after distorting map must obey:

$$b_h^{'} \le b_a^{'} \le b_e^{'} \tag{28}$$

Which relation can be shown as the thick dotted lines in figure 7(b). According to the formulas 26 and 28, we can deduce the constraint condition of 45^0 direction:

$$\begin{cases} Y_H - X_H - Y_A + X_A \le 0 \\ Y_A - X_A - Y_E + X_E \le 0 \end{cases} \tag{29}$$

The deduction of constraint criterion of -45^0 direction is just like the 45^0 direction constraint, the only difference is the plus-minus sign. So the -45^0 direction constraint condition is:

$$\begin{cases} Y_H + X_H - Y_A - X_A \le 0 \\ Y_A + X_A - Y_E - X_E \le 0 \end{cases} \tag{30}$$

And easily we also can get the 0^0 direction constraint:

$$\begin{cases} Y_H - Y_A \le 0 \\ Y_A - Y_E \le 0 \end{cases} \tag{31}$$

In the same way, the $\pm 90^0$ directions constraint is:

$$\begin{cases} X_H - X_A \le 0 \\ X_A - X_E \le 0 \end{cases} \tag{32}$$

4. Experiment design

In the section, we give a real urban service area map, including buildings, roads and some underground lines such as gas pipelines, water supplying pipelines and sewage lines. The original map is shown in figure 8(a). In such a figure, the data is coming from an area of a Chinese city. We analysis our method in two aspects: the level of simplifying and similarity.

4.1 Analysis of simplifying level

Simplifying level of a map is measured by its quantities of 8-directions edges. In figure 8(b) and figure 8(c), we compare our method with Stott's method, we can find that both methods are available for simplifying, making maps have fewer bends, and more artistic than original one.

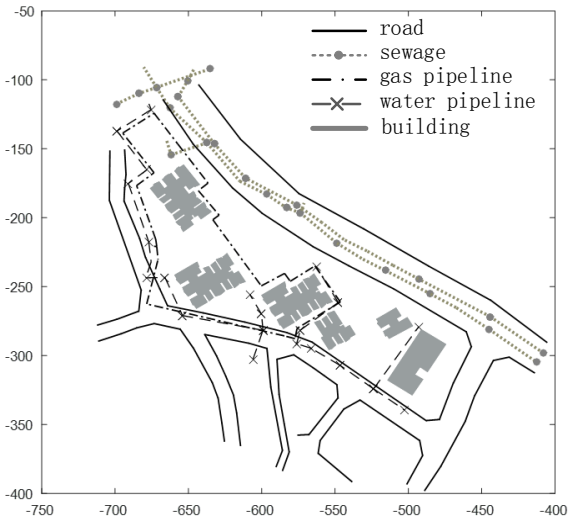

(a) The original map of a street area

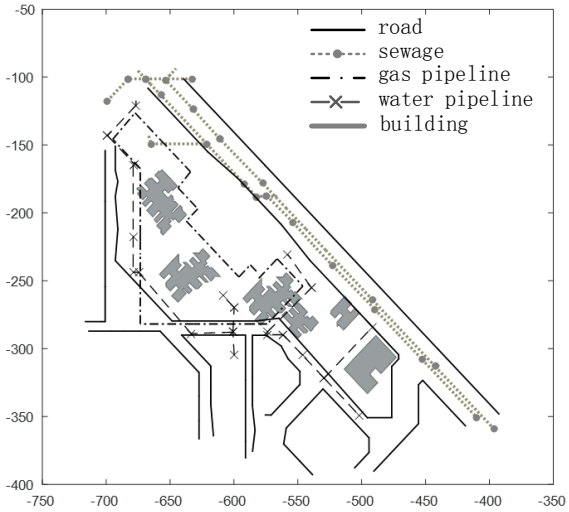

(b) The distorted map with Stott's method

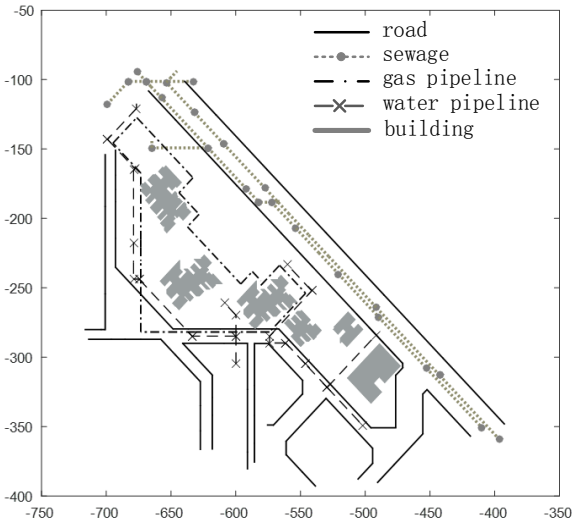

(c) The distorted map with our method

Fig.8 Compare between Stott's method and our method

However our method makes all the edges to be distributed in 8-directions when Stott's method just can keep a similar distribution. The reason is Stott's method is made by a set of relaxing constraints and any constraint accounts for just a part of the weight.

Our method builds a set of strict constraints, which are provided in inequations 6, 9, 21, 22, 23, 24, 29, 30, 31, 32. According these constraints, constructs a classic linear programming to solve the optimal value of the objective function. This linear programming includes known quantities such as each point j's original coordinate (x_j, y_j) and a pair of unknown quantities such as each point j's distorted coordinate (X_j, Y_j) and its dynamic grid radius R_j. Furthermore, as is shown in figure 8, our method give a special focus on the conflict avoidance among independent facilities in map, so little

conflict exists in figure 8(c), but much conflicts exist in figure 8(b). Our objective function is shown as following:

$$\min z = \sum_{j=1}^{n} R_j$$

(33)

In which function, n is the number of all the points in maps. The objective function means that we find an optimal value to keep the sum of each point's dynamic grid radius to be minimal.

4.2 Analysis of similarity level

Most research focuses on qualitative evaluation, in our experiment, we employ a quantitative evaluation which method is mentioned by professor Fu [21] in Wuhan University. This method choose a parameter named fractal dimension, which is an index to measure the similarity of two graphics.

This method obtains fractal dimension of a graphic by Box-counting [22]. With different size boxes which is shown in figure 9, the method counts the quantities of boxes which cover the target graphic. With this method, we can get a group of data in table 1. In order to compare 3 graphics in figure 8, we provide a set of line regressions of $lg\ Nr_i$ and $lg\ r_i$, which are shown in figure 9.

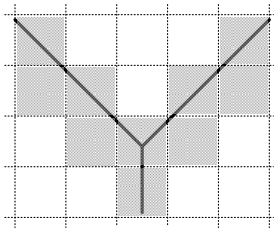

Fig.9 Box-counting method of fractal dimension

In table 1, there are 5 groups of data with different scales of box, r_i is the side length of a box, Nr_i is the total quantities of boxes when they cover the graphic. In such a table, when r_i is 1, $lg\ Nr_i$ of our graphic is 3.818622 which is more closer to original graphic value 3.820661 than this value of Stott's graphic which is 3.815245. Generally, our graphic is more similar to the original graphic than Stott's graphic in a quantitative evaluation. One of the reasons is that this paper chooses an optimal method, which makes sure all the points move the shortest length comparing to their original locations. Another reason is that this paper give a special attention on conflicts among

facilities, which would maintain the facilities' relative locations as the original graphic. According to fractal theory, the relation between r_i and Nr_i can be expressed as:

$$\lg Nr_i = A - D\lg r_i \tag{33}$$

Tab.1 Fractal dimension calculation table

Box scale (r_i)	$lg\ r_i$	Original graphic		Our graphic		Stott's graphic	
		Quantities of boxes (Nr_i)	$lg\ Nr_i$	Quantities of boxes (Nr_i)	$lg\ Nr_i$	Quantities of boxes (Nr_i)	$lg\ Nr_i$
1	0	6617	3.820661	6586	3.818622	6535	3.815245
4	0.602059	1400	3.146128	1347	3.129368	1339	3.126781
8	0.903089	585	2.767156	599	2.777427	606	2.782473
20	1.301209	141	2.149219	145	2.161368	145	2.161368
40	1.602059	45	1.653213	45	1.653213	46	1.662759

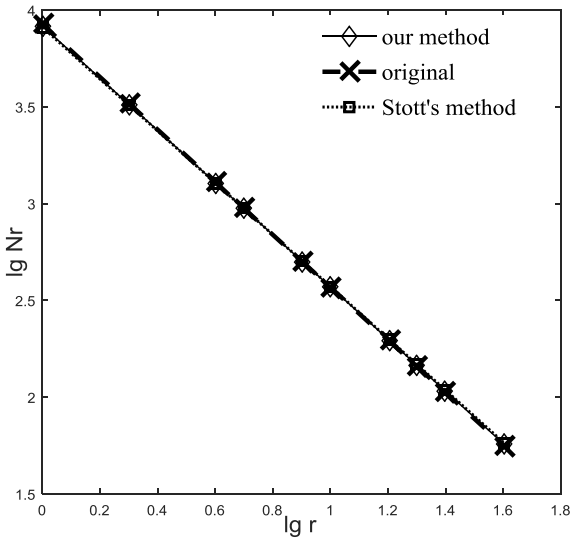

Fig.10 Fractal dimension compare among original map, Stott's map and our map

The parameter A is a constant, D is the fractal dimension of the graphic, in this place, fractal dimension is also called similarity dimension. Our experiment is to compare the similarity dimensions among those graphics in figure 8. In order to get the value of D, we acquire a set of r_i and Nr_i to achieve unary linear regression. This can be shown in figure 10, 3 graphics' similarity dimensions are much close, so our method and Stott's method are feasible. In table 2, we provide the Ds of 3 graphics in figure 10 particularly. It shows that our method can get a closer value of D to the original one than Stott's method.

Tab.2 Compare of similarity dimensions

Similarity dimension	Original graphic	Our graphic	Stott's graphic
D	-1.358326	-1.347578	-1.339893

5. Conclusion

This paper provides an effective schematic method based on dynamic grid to generate service area map automatically. The method includes a direction constraint to limit line's direction, a dynamic grid method to restrain 2 adjacent points, a specific orientation constraint and an independent-facilities relative location maintaining. These a set of methods cause a strict constraint on directions and locations. Furthermore, we verify our method both by qualitative evaluation and quantitative evaluation. The result shows that our method can generate a map with little conflict and bend than the Stott's method, and keep a better similarity than Stott's method mildly.

References

1. Z. Nougrara, Towards Robust Analysis of Satellite Images of Algeria Application to Road Network and its Nodes Extraction, 2015, AMSE Journals, vol. 28, no.1, pp.53-66.
2. Ping Wan, Kaiwen Luo, Application of Device Control and Manage Method in Military, 2016, Review of Computer Engineering Studies, vol. 3, no. 2, pp.29-33.
3. Klippel A, Richter K F, Barkowsky T, The Cognitive Reality of Schematic Maps, 2005, Map-based Mobile Services, Springer Berlin Heidelberg, pp.55-71.
4. Tversky B, Lee P U, Pictorial and Verbal Tools for Conveying Routes, 1999, Spatial Information Theory: Cognitive and Computational Foundations of Geographic Information Science, International Conference COSIT '99, 1999, Stade, Germany, pp.51-64.
5. Hadlaw J, The London Underground Map: Imagining Modern Time and Space, 2003, Design Issues, vol. 19, no. 1, pp.25-35.
6. Neyer G, Line Simplification with Restricted Orientations, 1999, Lecture Notes in Computer Science, vol. 1663, pp.13-24.
7. Merrick D, Gudmundsson J, Path Simplification for Metro Map Layout, 2006, International Conference on Graph Drawing, 2006, Berlin, Germany, pp.258-269.
8. Cabello S, Kreveld M V, Schematic Networks: An Algorithm and its Implementation, 2002, Advances in Spatial Data Handling, Springer Berlin Heidelberg, pp.475-486.

9. Cabello Justo S, De Berg M T, Van Kreveld M J, Schematization of Networks, 2005, Computational Geometry Theory & Applications, vol. 30, no. 3, pp.223-238.
10. Barkowsky T, Latecki L J, Kai F R, Schematizing Maps: Simplification of Geographic Shape by Discrete Curve Evolution, 2000, Lecture Notes in Computer Science, vol.1849, pp.41-53.
11. Oke O, Siddiqui S, Efficient automated schematic map drawing using multiobjective mixed integer programming, 2015, Computers & Operations Research, vol. 61, pp.1-17.
12. Ware J M, Taylor G E, Anand S, Automated Production of Schematic Maps for Mobile Applications, 2006, Transactions in Gis, vol. 10, no. 1, pp.25-42.
13. Anand S, Avelar S, Ware J M, Automated schematic map production using simulated annealing and gradient descent approaches, 2007, Proceedings of the 15th Annual GIS Research UK Conference, 2007, Dublin, Ireland, pp.11-13.
14. Hong S H, Merrick D, Nascimento Hadd, Automatic visualisation of metro maps, 2006, Journal of Visual Languages & Computing, vol. 17, no. 3, pp.203-224.
15. Stott J, Rodgers P, Martínezovando J C, Automatic Metro Map Layout Using Multicriteria Optimization, 2011, Visualization & Computer Graphics IEEE Transactions on, vol. 17, no. 1, pp.101-114.
16. Nöllenburg M, Wolff A, Drawing and Labeling High-Quality Metro Maps by Mixed-Integer Programming, 2010, Visualization & Computer Graphics IEEE Transactions on, vol. 17, no. 5, pp.626-641.
17. Regnauld N, Contextual Building Typification in Automated Map Generalization, 2001, Algorithmica, vol. 30, no. 2, pp.312-333.
18. J. H. Haunert and A. Wolff, Optimal and topologically safe simplification of building footprints, 2010, Sigspatial International Conference on Advances in Geographic Information Systems, 2010, ACM, pp.192-201.
19. Li Zhenhua, Yang Chuncheng, Wei Fu, A displacement algorithm based on geometry similarity for spatial conflicts between roads and buildings, 2016, Acta Geodaetica et Cartographica Sinica, vol. 45, no. 6, pp.747-755.
20. Ti P, Li Z, Generation of schematic network maps with automated detection and enlargement of congested areas, 2014, International Journal of Geographical Information Science vol. 28, no. 3, pp.521-540.
21. Fu Zhongliang, Weng Baofeng, Hu Yulong, A schematic method based on the integration of stroke construction and displacement for road network, 2016, Acta Geodaetica et Cartographica Sinica, vol. 45, no. 9, pp.1115-1121.

22. Sarkar N, Chaudhuri B B, An efficient differential box-counting approach to compute fractal dimension of image, 1994, IEEE Transactions on Systems Man & Cybernetics, vol. 24, no. 1, pp.115-120.